ARTICLE IN PRESS

Digital Communications and Networks xxx (xxxx) xxx

Contents lists available at ScienceDirect

Digital Communications and Networks

journal homepage: www.keaipublishing.com/dcan

Resource allocation for sum-rate maximization in NOMA-based generalized spatial modulation

Guoquan Li [a,b], Zijie Hong [a,b], Yu Pang [b,*], Yongjun Xu [a], Zhengwen Huang [c]

[a] School of Communication and Information Engineering, Chongqing University of Posts and Telecommunications, Chongqing, 400065, China
[b] Chongqing Key Laboratory of Photoelectronic Information Sensing and Transmitting Technology, Chongqing, 400065, China
[c] Department of Electronic and Electrical Engineering, Brunel University London, London, UB8-3PH, UK

ARTICLE INFO

Keywords:
Resource allocation
NOMA
Spatial modulation
Power allocation
User grouping

ABSTRACT

The Multiple-input Multiple-output (MIMO) Non-orthogonal Multiple Access (NOMA) based on Spatial Modulation (SM-MIMO-NOMA) system has been proposed to achieve better spectral efficiency with reduced radio frequency chains comparing to the traditional MIMO-NOMA system. To improve the performance of SM-MIMO-NOMA systems, we extend them to generalized spatial modulation scenarios while maintaining moderate complexity and fairness. In this paper, system spectral efficiency and transmission quality improvements are proposed by investigating a sum-rate maximization resource allocation problem that is subject to the total transmitted power, user grouping, and resource block constraints. To solve this non-convex and difficult problem, a graph-based user grouping strategy is proposed initially to maximize the mutual gains of intragroup users. An auxiliary-variable approach is then adopted to transform the power allocation subproblem into a convex one. Simulation results demonstrate that the proposed algorithm has better performance in terms of bit error rate and sum rates.

1. Introduction

In future Beyond Fifth-Generation (B5G) mobile communication networks, many technologies will be widely investigated and researched, such as fog-computing-enabled mobile communication networks [1] and open networks featuring with convergence of communication, computing and caching [2]. Among urgent considerations are the expectations that higher user or device capacity, lower cost, and higher spectral utilization will be addressed. Non-orthogonal Multiple Access (NOMA) [3,4] is one of the candidate technologies that has demonstrated its capacity to improve the spectral efficiency or transmission rate in B5G networks [5]. Moreover, system complexity is another important consideration, especially for Multiple-input Multiple-output (MIMO) scenarios with large numbers of transmit antennas. Hardware costs increase with increasing number of users in MIMO-NOMA systems [6]. For resolving the above issues, Spatial Modulation (SM) technology [7] was introduced to MIMO-NOMA systems, namely, SM-MIMO-NOMA systems [8–10].

Although traditional SM-MIMO-NOMA systems can allow users to utilize power domain resources with reduced Radio Frequency (RF) chains, system performance is severely affected by the SM mapper rule, which ensures that there can only be one active transmit antenna. However, Generalized Spatial Modulation (GSM), as an extended SM technology, can allow users to select multiple active transmit antennas [11–14]. Consequently, the combination of GSM and MIMO-NOMA (GSM-MIMO-NOMA) systems becomes an effective approach for high spectral utilization while maintaining moderate complexity and fairness. Moreover, different demands in a GSM-MIMO-NOMA system can be effectively satisfied by dynamic resource allocation schemes, including user grouping and power allocation [15].

1.1. Related works

Studies on traditional NOMA systems can be mainly classified into three different types: user grouping; power allocation; and joint user grouping and power allocation.

1.1.1. User grouping

In [16], random user grouping was studied to meet various Quality of Service (QoS) requirements in MIMO-NOMA systems. In Ref. [17], a sum-rate maximization problem with service rate constraints was considered to produce quality-balanced user grouping schemes. In

* Corresponding author.
E-mail address: pangyu@cqupt.edu.cn (Y. Pang).

https://doi.org/10.1016/j.dcan.2022.02.005
Received 29 July 2020; Received in revised form 30 December 2021; Accepted 20 February 2022
Available online xxxx

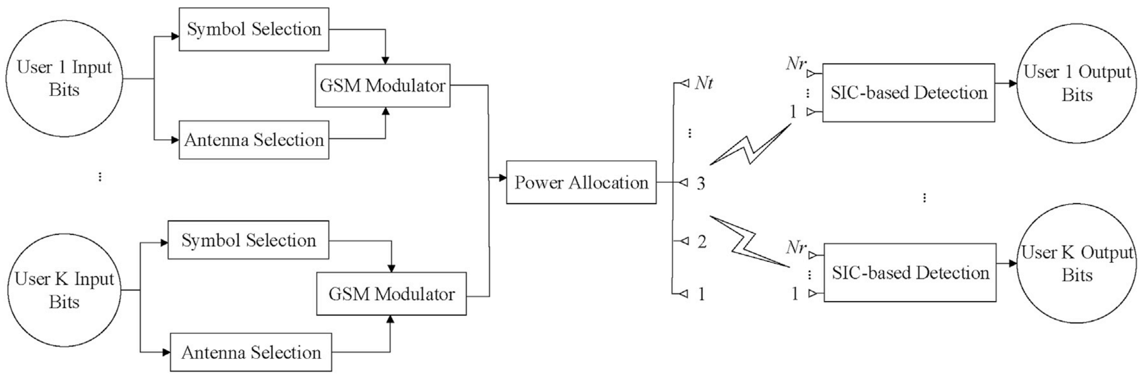

Fig. 1. GSMN system illustration.

Ref. [18], an energy minimization-based user grouping for NOMA-assisted Multi-access Edge Computing (MEC) systems was proposed using matching theory.

1.1.2. Power allocation

Iterative power allocation algorithms were proposed to reduce outage probabilities in uplink NOMA systems [19], to improve energy efficiency in downlink NOMA systems [20], and to guarantee fairness in uplink and downlink NOMA systems [21,22]. The gradient ascent method and gradient descent method were presented to maximize the Achievable Sum Rate (ASR) in NOMA-millimeter wave systems [23]. Moreover, a non-convex power allocation problem with QoS requirements was studied, utilizing Successive Convex Approximation (SCA) in downlink NOMA systems [24]. Furthermore, the robust interference efficiency maximization problem was investigated in heterogeneous networks [25,26].

1.1.3. Joint user grouping and power allocation

In downlink NOMA systems, a multiuser user grouping scheme was proposed to improve the ASR, and an optimal power allocation scheme was designed to outperform conventional Orthogonal Multiple Access (OMA) systems [27]. In uplink and downlink NOMA systems, the problem of throughput maximization was discussed by Refs. [28,29], utilizing the Lagrangian multiplier method and the Karush-Kuhn-Tucher condition. In uplink massive MIMO-NOMA systems, a sum-rate maximization problem was studied by Ref. [30], where efficient user grouping and power allocation algorithms were proposed under received power constraints.

There are several prior works on SM-MIMO-NOMA systems. Spectral efficiency was analyzed by Refs. [8,10], and the Bit Error Rate (BER) was studied by Ref. [9] where random user grouping and fixed power allocation schemes were considered. However, dynamic user grouping and power allocation were investigated for SM-MIMO-NOMA systems to improve the ASR, achieving significant performance enhancement in comparison with random grouping and fixed power allocation [31]. Furthermore, MIMO-NOMA systems based on quadrature spatial modulation were designed [15] where the real and imaginary parts of a symbol were separated for transmission and an iteration method was employed to obtain better user grouping and power allocation. Moreover, the spatial multiple access system was proposed to reduce the complexity of NOMA systems by Ref. [32]. Furthermore, MIMO-NOMA systems based on generalized space shift keying were proposed, where some users utilized power domain resources and others used spatial domain resources [33].

1.2. Motivation

Unlike [8–10], existing works have considered two-user SM-MIMO-NOMA systems. However, such systems waste spatial domain resources and cannot satisfy demand for massive connectivity. Consequently, multiuser GSM-MIMO-NOMA systems can be considered for downlink scenarios. Traditional schemes are too ideal to meet differing requirements, and intragroup gain maximization cannot be guaranteed. Moreover, the power allocation coefficient is fixed regardless of channel conditions, as noted by Refs. [8–10]. Moreover, Best-near Best-far (BNBF) user grouping [34], fixed two-user power allocation [32], and QoS-based power allocation [35,36] cannot achieve a tradeoff between system performance and complexity. Motivated by these problems, dynamic resource allocation is required to achieve sum-rate maximization for GSM-MIMO-NOMA systems.

1.3. Contributions and organization

In this paper, we consider a downlink GSM-MIMO-NOMA system. The sum-rate maximization resource allocation problem is studied under the consideration of a total transmit power constraint, a user grouping constraint, and a resource block constraint. The main contributions are outlined as follows:

- A GSM-MIMO-NOMA system is investigated, where two or more symbols are sent by the Transmit Antenna Combination (TAC), which is based on the GSM mapping rule. Moreover, mutual interference coming from other transmit antennas has been considered by the Maximum Likelihood (ML) detection, and intragroup interference could be mitigated by a Successive Interference Cancellation (SIC) procedure. Therefore, a GSM-MIMO-NOMA system achieves a better trade-off between spectral efficiency and complexity in comparison to other existing systems.
- The non-convex resource allocation problem is difficult to solve because optimized variables become entangled with each other. To resolve this problem, a graph-based user grouping strategy is proposed to initially achieve mutual gain maximization in intragroup users, where the min-cut problem is considered. An auxiliary-variable approach is then adopted to transform the power allocation subproblem into a convex one.
- Comprehensive experiments and fair comparisons are performed to show how BER and ASR are improved with different Signal-to-Noise Ratios (SNRs), numbers of reception antennas, and number of users.

The rest of this paper is organized as follows: Section 2 presents system model and problem formulation; Sections 3 and 4 discuss the user grouping strategy and power allocation strategy, respectively; Section 5 shows simulation results and performance analysis; And conclusions are drawn in Section 6.

Notation: $(\cdot)^H$ is the conjugate transpose operation, $tr(\cdot)$ denotes the trace operation, $\lfloor \cdot \rfloor$ is the floor operation, $\| \cdot \|^2$ denotes the second-order norm operation, ${}_nC_k$ is the binomial coefficient of $[n, k]$, $\mathbb{C}$ denotes a complex number field, $\mathbb{Z}$ is an integer field, $\mathrm{Re}(\cdot)$ denotes the real part of

Table 1
Symbol notations.

Symbol	Definition
$\mathbf{H}_i^t$	The channel matrix of u_i^t
$\mathbf{H}_{i,\mathbf{J}_i^t}^t$	The $(\mathbf{J}_i^t)^{th}$ column of $\mathbf{H}_i^t$ of u_i^t
$\gamma_{i,\mathbf{J}_i}^t$	The effective channel gain for $\mathbf{H}_{i,\mathbf{J}_i^t}^t$ of u_i^t
$\mathbf{x}_{i,\mathbf{J}_i^t}^t$	The transmitted signal of u_i^t with the chosen TAC $\mathbf{J}_i^t$
s_i^t	The APM symbol of u_i^t
$\mathbf{s}_i^t$	The effective symbol vector of u_i^t
$\mathbf{y}_i^t$	The received signal of u_i^t

Table 2
The mapping rule of the GSM-MIMO-NOMA system.

Input bit	TAC	APM symbols	Input bit	TAC	APM symbols
0000	(1, 3)	(+1, +1)	1000	(2, 4)	(+1, +1)
0001	(1, 3)	(+1, −1)	1001	(2, 4)	(+1, −1)
0010	(1, 3)	(−1, +1)	1010	(2, 4)	(−1, +1)
0011	(1, 3)	(−1, −1)	1011	(2, 4)	(−1, −1)
0100	(1, 4)	(+1, +1)	1100	(2, 3)	(+1, +1)
0101	(1, 4)	(+1, −1)	1101	(2, 3)	(+1, −1)
0110	(1, 4)	(−1, +1)	1110	(2, 3)	(−1, +1)
0111	(1, 4)	(−1, −1)	1111	(2, 3)	(−1, −1)

the complex number, and $\mathcal{CN}(\mu,\sigma)$ is complex Gaussian distribution with mean μ and variance σ^2.

2. System model and problem formulation

2.1. Proposed SM-MIMO-NOMA system

Consider a downlink GSM-MIMO-NOMA system one Base Station (BS) with N users. Assume that the BS is equipped with N_t transmit antennas and each user has N_r reception antennas, where N_a transmit antennas are chosen in each time slot. Given a number of groups T and a number of users K in each group, the total number of users is $N = KT$. Define u_i^t as the i^{th} user of the t^{th} group, $i \in \{1, 2, \ldots, K\}$, and $t \in \{1, 2, \ldots, T\}$. Moreover, the total amount of resources is Φ, and the number of resource blocks allocated to the t^{th} group is represented by φ_t, where $1 \le \varphi_t \le \Phi$. Furthermore, NOMA is implemented within each group and different groups are assigned to orthogonal resources (i.e., intergroup interference can be eliminated by adopting OMA among different groups, as in Refs. [8,10]). Taking a group $\mathcal{G}$ as an example, the GSM-MIMO-NOMA system model is shown in Fig. 1. System symbols are presented in Table 1. In the GSM-MIMO-NOMA system, both the Rayleigh fading and path loss are considered as $\mathbf{H}_i^t = d_{i,t}^{-\alpha}\tilde{\mathbf{H}}_i^t \in \mathbb{C}^{N_r\times N_t}$, where $\mathbf{H}_i^t$ is the channel matrix of u_i^t, $d_{i,t}$ is the distance between the BS and u_i^t, and the path loss exponent is indicated by α [34]. $\tilde{\mathbf{H}}_i^t$ is the Rayleigh fading coefficient from the BS to u_i^t with entries that are independent and identically distributed (i.i.d.) as $\mathcal{CN}(0,1)$ [9].

The number of TACs is $N_c = 2^{\lfloor \log_2({}_{N_t}C_{N_a})\rfloor}$, where ${}_{N_t}C_{N_a}$ is the binomial coefficient of $[N_t, N_a]$. The set of all TACs is $\Gamma = \{\mathbf{I}_1, \ \mathbf{I}_2, \ \cdots, \ \mathbf{I}_{N_c}\}$, where $\mathbf{I}_i \in \mathbb{Z}^{N_a\times 1}$ is the i^{th} TAC. When $N_t = 4$ and $N_a = 2$ are given, $N_c = 4$ is derived. In this instance, there are six ways (i.e., six possible TACs) to choose two active antennas from four transmit antennas, making the set of six possible TACs $\{(1,2),(1,3),(1,4),(2,3),(2,4),(3,4)\}$ from which we can arbitrarily select four TACs, such as $\{(1,3),(2,4),(1,4),(2,3)\}$, as in Ref. [12]. However, in this paper, $\Gamma = \{\mathbf{I}_1, \ \mathbf{I}_2, \ \mathbf{I}_3, \ \mathbf{I}_4\} = \{(1,3),(1,4),(2,4),(2,3)\}$ is assumed, where two successive TAC differ in only one index of transmit antennas rather than two indices of transmit antennas, as in the traditional schemes used in Ref. [12].[1] In Table 2, the mapping rule of the GSM-MIMO-NOMA system with $N_t = 4$ and $N_a = 2$ is defined, where the Binary Phase-shift Keying (BPSK) modulation is used.

Therefore, the transmitted signal of u_i^t is defined as follows:

$$\mathbf{x}_{i,\mathbf{J}_i^t}^t = \begin{bmatrix} 0 & s_{i,1}^t & \cdots & s_{i,N_a}^t & 0 \end{bmatrix}^T \qquad \begin{matrix} \uparrow j_{i,1}^t & \cdots & \uparrow j_{i,N_a}^t & position \end{matrix} \tag{1}$$

where $\mathbf{J}_i^t \in \mathbb{Z}^{N_a\times 1}$ denotes the chosen TAC of u_i^t, including different N_a transmit antennas from $j_{i,1}^t$ to j_{i,N_a}^t, $s_{i,m}^t \in \mathbb{C}^{1\times 1}$ is the Amplitude and Phase Modulation (APM) symbol of u_i^t at the $j_{i,m}^t$ position, given that $1 \le m \le N_a$. $\mathbf{x}_{i,\mathbf{J}_i^t}^t \in \mathbb{C}^{N_t\times 1}$ shows the transmitted signal of u_i^t, the non-zero values of $\mathbf{x}_{i,\mathbf{J}_i^t}^t$ denote the APM symbols of N_a active transmit antennas, and other elements of $\mathbf{x}_{i,\mathbf{J}_i^t}^t$ present the symbols of silent transmit antennas.

N_a different APM symbols are sent by N_a different transmit antennas. Therefore, the combination of N_a different APM symbols can be named as the effective symbol vector:

$$\mathbf{s}_i^t = \left[s_{i,1}^t \ s_{i,2}^t \cdots s_{i,N_a}^t\right]^T \tag{2}$$

where $\mathbf{s}_i^t \in \mathbb{C}^{N_a\times 1}$ denotes the effective symbol vector of u_i^t.

Without a loss of generality, $||\mathbf{H}_1^t||^2 > ||\mathbf{H}_2^t||^2 > \cdots > ||\mathbf{H}_K^t||^2$, where $\mathbf{H}_i^t \in \mathbb{C}^{Nr\times N_t}$ is the channel matrix of u_i^t. Thus, the first user is the closest user to the BS; as such, the BS will allocate less power to that user, as in Ref. [28].

Therefore, the received signal of u_i^t can be expressed as

$$\mathbf{y}_i^t = \sqrt{\frac{\beta_i^t P}{N_a}}\mathbf{H}_{i,\mathbf{J}_i^t}^t\mathbf{s}_i^t + \underbrace{\sum_{k\neq i}^{K}\sqrt{\frac{\beta_k^t P}{N_a}}\mathbf{H}_{i,\mathbf{J}_k^t}^t\mathbf{s}_k^t}_{\text{intragroup interference}} + \mathbf{w}_i^t \tag{3}$$

where P is the total transmitted power, β_i^t is the power allocation coefficient of u_i^t, $\mathbf{y}_i^t \in \mathbb{C}^{N_r\times 1}$ is the received signal of u_i^t, $\mathbf{H}_{i,\mathbf{J}_i^t}^t \in \mathbb{C}^{N_r\times N_a}$ is the $(\mathbf{J}_i^t)^{th}$ column of the channel matrix $\mathbf{H}_i^t$ of u_i^t, and $\mathbf{w}_i^t \in \mathbb{C}^{N_r\times 1}$ is the additive white Gaussian noise with its i.i.d. entries $\mathcal{CN}(0,\sigma^2)$. Moreover, $\mathbf{H}_{i,\mathbf{J}_i^t}^t\mathbf{s}_i^t = \sum_{m=1}^{N_a}\mathbf{H}_{i,j_{i,m}^t}^t s_{i,m}^t$, which includes the mutual interference coming from different antennas of u_i^t.

The data rate of u_i^t of the proposed GSMN systems is

$$L_i^t = \lfloor \log_2\left({}_{N_t}C_{N_a}\right)\rfloor + N_a\log_2(M) \tag{4}$$

where the first $\lfloor\log_2({}_{N_t}C_{N_a})\rfloor$ bit is utilized for selecting the TAC, and the remaining $N_a\log_2(M)$ bit is used for determining APM symbols [11,12].

Moreover, the ASR of the GSM-MIMO-NOMA system is defined as $R_{sum} = \sum_{t=1}^{T}\sum_{i=1}^{K}R_i^t$, where R_{sum} is the ASR of the GSMN system, and R_i^t is the achievable rate of u_i^t as

$$R_i^t = \begin{cases} \log_2\left(1 + \dfrac{\beta_1^t P\gamma_{1,\mathbf{J}_1}^t}{N_a\sigma^2}\right), \ i = 1, \\ \log_2\left(1 + \dfrac{\beta_i^t P\gamma_{i,\mathbf{J}_i}^t}{\sum\limits_{k=1}^{i-1}\beta_k^t P\gamma_{i,\mathbf{J}_k}^t + N_a\sigma^2}\right), \ otherwise \end{cases} \tag{5}$$

where $\gamma_{i,\mathbf{J}_i}^t = tr(\mathbf{H}_{i,\mathbf{J}_i^t}^t(\mathbf{H}_{i,\mathbf{J}_i^t}^t)^H)$ is the effective channel gain of u_i^t in the GSM-MIMO-NOMA system. Furthermore, in this paper, detection is based on ML detection with the SIC procedure, as in Ref. [9]. Moreover, the detection processes is based on perfect Channel State Information (CSI) at the receiver [9], making this ideal model without having to consider imperfect CSI to avoid the existence of channel uncertainties

[1] The impact of antenna selection on the performance of SM-MIMO-NOMA/GSM-MIMO-NOMA systems is beyond the scope of this paper. However, these will be considered in our future work.

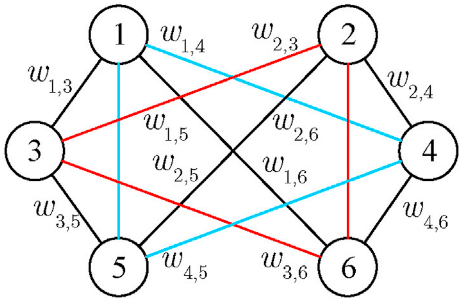

Fig. 2. Graph representation of the gain relation for users in GSM-MIMO-NOMA systems with $K = 2$ and $T = 3$.

because of channel estimation errors.

2.2. Problem formulation

For a significant performance improvement in GSM-MIMO-NOMA systems, a joint user grouping and power allocation problem for ASR maximization can be considered. Therefore, this problem is formulated as

$$
\begin{aligned}
&\max_{\beta_i^t,\mu_i^t} \quad \sum\nolimits_{t=1}^{T}\sum\nolimits_{i=1}^{N}\mu_i^t \log_2\left(1+\frac{\beta_i^t P\gamma_{i,\mathbf{J}_i}^t}{\sum\limits_{k\neq i}\mu_k^t\beta_k^t P\gamma_{i,\mathbf{J}_i}^t + N_a\sigma^2}\right)\\
&s.t. \quad C_1:\ \sum\nolimits_{i=1}^{N}\mu_i^t\beta_i^t P = P, \quad \forall t\\
&\qquad C_2:\ \sum\nolimits_{i=1}^{N}\mu_i^t\beta_i^t = 1, \quad \forall t\\
&\qquad C_3:\ \sum\nolimits_{t=1}^{T}\mu_i^t = 1, \quad \mu_i^t\in\{0,\ 1\}, \quad \forall i,\ t\\
&\qquad C_4:\ \sum\nolimits_{i=1}^{N}\mu_i^t = N/T, \quad \forall t
\end{aligned}
\tag{6}
$$

where C_1 is the maximum transmitted power constraint, C_2 is the power allocation coefficient constraint, C_3 indicates that one user can be selected by one group at most, $\mu_i^t = 1$ and $\mu_i^t = 0$ denote that the user is, or is not, respectively involved with a group, and C_4 represents the number of intragroup user constraints.

The problem mentioned above is mixed integer and nonlinear programming [28]. For ASR maximization, an exhaustive search is adopted to find the optimal user grouping solution, where the number of searches for optimal user grouping can be represented as $\prod_{i=1}^{T}[_{(N\ (i\ 1)K)}C_K-(i-1)K)] = \frac{(KT)!}{K^T}$ [37], but the optimal solution may be difficult or infeasible to solve for practical systems (e.g., if N is very large).

To solve this problem, we propose a low-complexity two-step method that will perform user grouping followed by power allocation for each group. In this way, a suboptimal solution can be found while maintaining lower complexity.

3. User grouping strategy

In this section, a low-complexity suboptimal user grouping strategy is proposed for GSM-MIMO-NOMA systems, namely, min-cut grouping, which is based on the min-cut problem in graph theory. Traditional schemes include the best-near worst-far user grouping [29] and BNBF user grouping [34]. However, these schemes only consider two-user grouping results. User grouping schemes can be translated into graph-based optimization problems. In vehicular communication networks, vehicles are divided into different clusters to minimize intergroup interference where a graph-based algorithm was exploited [38]. However, in GSM-MIMO-NOMA systems, performance enhancement can be achieved by optimizing the sum of gains for intragroup users (mutual gains). To maximize these mutual gains, users with lower gains should be divided into different groups. Therefore, a min-cut algorithm should be exploited to place users with weaker mutual gains in different groups, allowing all users in any given group to achieve mutual gain maximization.

Suppose there are T initial sets, and each initial set has K users. Then, constraints C_3 and C_4 of (6) should be satisfied.

The mutual gain relation of users can be expressed by an undirected graph, Fig. 2, where a vertex denotes a user and two vertices are joined by an edge. The edge weight $\omega_{a,b} = \gamma_{a,\mathbf{J}_a}^{t_a} + \gamma_{b,\mathbf{J}_b}^{t_b}$ indicates the mutual gain level between users a and b from initial sets t_a and t_b, respectively. The objective is to minimize the total weight of edges in different groups. The min-cut user grouping strategy is equivalent to the min-cut problem in graph theory, which is described briefly below. Given a graph $G = (V, E)$, the vertex set is V, i.e., the set of all users. V_i denotes the set of users in the i^{th} initial set. Moreover, the edge set is E and the set of edges to be selected $E_i \subseteq V_i \times V_i$, where V_i is the complementary set of V_i, and $1 \le i \le T$. Thus, $E_i = \{e_{a,b} \in E;\ a \in V_i; b \in V - V_i\},(i = 1),E_i = \{e_{a,b} \in E - \sum_{j=1}^{i-1} E_j; a \in V_i; b \in V - \sum_{k=1}^{i} V_k\},(2 \le i < T)$.

Algorithm 1. Min-cut Grouping Procedure

Algorithm 1 Min-cut Grouping Procedure

Input: $\bar{T} = K, \bar{K} = T, V_i, i = 1, 2, \cdots, K; \gamma_{v,\mathbf{J}_v}, v \in V$;
Output: grouping results G_t where $t = 1, 2, \cdots, T$;
for $t = 1$ to T **do**
  while $(V_i > 0)$ and (length(V_i)> 0) **do**
    find $\arg\max_{a_i \in V_i} \omega_{a_1,a_2,\cdots,a_K}$;
    remove a_i coming from V_i to G_t;
    rename the users coming from V_i to u_i^t;
    where $i = 1, 2, \cdots, K$;
  end while
end for
return G_t where $t = 1, 2, \cdots, T$;

The min-cut problem for an undirected graph is to identify a partition of graph G into T disjoint groups G_t, where $1 \le t \le T$ and $G_1 \cup G_2 \cup \cdots \cup G_T = V$. Therefore, $T = K$ and $K = T$. Furthermore, we have

$$
\sum\nolimits_{i=1}^{T}\sum_{a,b\in G_t}\omega_{a,b} + \sum_{a'\in G_i, b'\in G_j, i\neq j}\omega_{a',b'} = \sum_{e\in E}\omega(e) \tag{7}
$$

This makes minimizing $\sum_{a'\in G_i, b'\in G_j, i\neq j}\omega_{a',b'}$ equivalent to maximizing $\sum_{i=1}^{T}\sum_{a,b\in G_t}\omega_{a,b}$. This also indicates that the min-cut grouping will determine the maximum sum of the weight of edges among users from different initial sets. In this way, users in a given group have a stronger total mutual gain than users in different groups, guaranteeing the mutual gain maximization in each group. For K-user grouping, we can compute the K-dimensional mutual gain $\omega^K = (K-1)\sum_{i=1}^{K}\gamma_{a_i,\mathbf{J}_{a_i}}^{t_{a_i}}$. Accordingly, Proposition 1 is obtained below.

Proposition 1. *If we select K users for a group, which includes the a_1^{th} user to the a_K^{th} user ($a_i \in V_i$), we can compute $w_{a_1,a_2,\ldots,a_K}$ instead of the sum of the edge weight intended for all grouping possibilities, guaranteeing the total mutual gain maximization in this group.*

Proof.. For $\forall K$, T, $a_i \in V_i$, $i = 1, 2, \ldots, K$, and any given K users that include the a_1^{th} user to the a_K^{th} user, we have

$$\begin{aligned}\omega^K &= \omega_{1,2}+\omega_{1,3}+\cdots+\omega_{1,K}+\omega_{2,3}+\cdots+\omega_{K-1,K}\\ &= \gamma^{t_{a_1}}_{a_1,\mathbf{J}_{a_1}}+\gamma^{t_{a_2}}_{a_2,\mathbf{J}_{a_2}}+\gamma^{t_{a_1}}_{a_1,\mathbf{J}_{a_1}}+\gamma^{t_{a_3}}_{a_3,\mathbf{J}_{a_3}}\\ &\quad+\cdots+\gamma^{t_{a_1}}_{a_1,\mathbf{J}_{a_1}}+\gamma^{t_{a_K}}_{a_K,\mathbf{J}_{a_K}}+\gamma^{t_{a_2}}_{a_2,\mathbf{J}_{a_2}}\\ &\quad+\gamma^{t_{a_3}}_{a_3,\mathbf{J}_{a_3}}+\cdots+\gamma^{t_{a_{K-1}}}_{a_{K-1},\mathbf{J}_{a_{K-1}}}+\gamma^{t_{a_K}}_{a_K,\mathbf{J}_{a_K}}\\ &= (K-1)\sum_{i=1}^{K}\gamma^{t_{a_i}}_{a_i,\mathbf{J}_{a_i}}\end{aligned} \tag{8}$$

Therefore, the proof of Proposition 1 is concluded.

4. Power allocation strategy

Consider a suboptimal power allocation strategy targeting sum-rate maximization, named MaxASR, for the proposed GSM-MIMO-NOMA system that differs from the target of satisfying the min-rate requirements by iteration, as in Ref. [15]. Suppose there are K users in each group and that the power allocation scheme is based on the assumption of the gain sort as in Section 2 [29]. Suppose the grouping result mentioned above is t^*. To improve the ASR of the GSM-MIMO-NOMA system, a max ASR problem is formulated as

$$\begin{aligned}&\max_{\beta_i^{t^*}}\ \sum\nolimits_{i=1}^{K}\log_2\Big(1+\frac{\beta_i^{t^*}P\gamma^{t^*}_{i,\mathbf{J}_i}}{\sum_{k=1}^{i-1}\beta_k^{t^*}P\gamma^{t^*}_{i,\mathbf{J}_k}+N_a\sigma^2}\Big)\\ &\qquad s.t.\ \ \sum\nolimits_{i=1}^{K}\beta_i^{t^*}=1\end{aligned} \tag{9}$$

where the constraint is the power allocation coefficient constraint.

This constraint is convex, but the objective function is non-convex because of the coupling between optimization variables in the objective function. There is an auxiliary variable approach [28,39] that identifies solutions by introducing an auxiliary variable $c_i^{t^*}$ in the following manner.

For the power allocation problem with constraints, it is difficult to find solutions with simple calculations, but there are existing algorithms that can produce solutions by introducing an auxiliary variable:

$$c_i^{t^*}\le\Big(1+\frac{\beta_i^{t^*}P\gamma^{t^*}_{i,\mathbf{J}_i}}{I^{t^*}_{i,\mathbf{J}_i}}\Big) \tag{10}$$

where $I^{t^*}_{i,\mathbf{J}_i}=\sum_{k=1}^{i-1}\beta_k^{t^*}P\gamma^{t^*}_{i,\mathbf{J}_k}+\sigma^2$ is the sum of interference and noise at $u_i^{t^*}$.

By maximizing $\prod_{i=1}^{K}c_i^{t^*}$ instead, the power allocation problem is translated as:

$$\begin{aligned}&\max_{\beta_i^{t^*},c_i^{t^*}}\quad \prod\nolimits_{i=1}^{K}c_i^{t^*}\\ &s.t.\quad C_1:\ \sum\nolimits_{i=1}^{K}\beta_i^{t^*}=1\\ &\qquad C_2:\ \frac{c_i^{t^*}I^{t^*}_{i,\mathbf{J}_i}}{I^{t^*}_{i,\mathbf{J}_i}+\beta_i^{t^*}P\gamma^{t^*}_{i,\mathbf{J}_i}}\le 1\\ &\qquad C_3:\ c_i^{t^*}>0\end{aligned} \tag{11}$$

where C_1 is similar to (9), C_2 and C_3 are the upper bound and the lower bound constraint of the auxiliary variable, respectively. Since the objective function and the constraints are posynomials, (11) is geometric programming [39].

By introducing variable substitution and replacing variables β_i^t and c_i^t by $e_i^{\beta}t$ and $e_i^{c}t$, respectively, this problem can be translated into convex programming. As C_2 is a non-convex constraint on variables β_i^t and c_i^t, the problem can be determined by taking the logarithm of C_2 at both sides, using exponential transformation as in Ref. [39], and convert it into a convex state. Thus, the constraint C_2 can be changed to

$$\ln(e^{c_i^{t^*}}I^{t^*}_{i,\mathbf{J}_i})-\ln(I^{t^*}_{i,\mathbf{J}_i}+e^{\beta_i^{t^*}}P\gamma^{t^*}_{i,\mathbf{J}_i})\le 0 \tag{12}$$

Therefore, (11) can be translated into

$$\begin{aligned}&\max_{\beta_i^{t},c_i^{t}}\quad \prod\nolimits_{i=1}^{K}c_i^{t^*}\\ &s.t.\quad C_1:\ \sum\nolimits_{i=1}^{K}\beta_i^{t^*}=1\\ &\qquad C_2:\ ln(e^{c_i^{t^*}}I^{t^*}_{i,\mathbf{J}_i})-\ln(I^{t^*}_{i,\mathbf{J}_i}+e^{\beta_i^{t^*}}P\gamma^{t^*}_{i,\mathbf{J}_i})\le 0\\ &\qquad C_3:\ c_i^{t^*}>0\end{aligned} \tag{13}$$

where C_2 is a convex constraint. At this point, this optimization problem is convex, rendering it solvable using an unmodified solver (e.g., CVX) [40].

Table 3
Simulation schemes.

Scheme	User grouping	Power allocation
Scheme 1	Min-cut grouping	MaxASR strategy
Scheme 2	Min-cut grouping	QoS-based strategy of [35,36]
Scheme 3	Min-cut grouping	SIC-based strategy of [9]
Scheme 4	Min-cut grouping	Fixed two-user strategy of [32]
Scheme 5	BNBF grouping of [34]	MaxASR strategy
Scheme 6	MaxRate grouping of [37]	MaxASR strategy
Scheme 7	Random grouping	Fixed two-user strategy of [32]
Scheme 8	Random grouping	Fixed three-user strategy

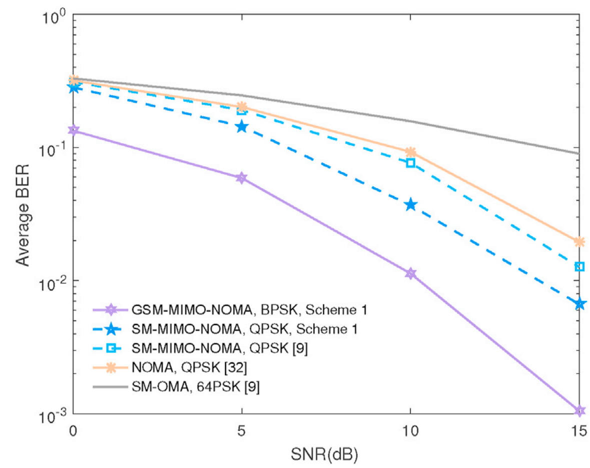

Fig. 3. Average BER performance of different two-user 4 × 4 systems with $K=2$, $T=6$, $P=1$, $\alpha=3$, and $R=4$ bits/symbol.

5. Simulation results

5.1. Performance analysis

Our simulation results demonstrated the effectiveness of proposed GSM-MIMO-NOMA schemes by comparing them with SM-OMA, MIMO-NOMA, and SMN schemes. To ensure a fair comparison, we started by considering a two-user SM-MIMO-NOMA/GSM-MIMO-NOMA case, then presenting results for a three-user case. For these cases, we assume a total $N=12$ users in all systems, where two-user systems have $T=6$ groups and three-user systems have $T=4$ groups. Given that the total power P of each group is fixed, as in Refs. [9,37], the noise power of all users is σ^2, and $\varphi_l=1$, $\forall l$. In addition, our simulation results were generated by averaging over 10,000 independent channel realizations.

After choosing a proper modulation mode, a data stream is modulated at the sender, with a data part being mapped to the antenna sequence number and another part being mapped to the constellation diagram; the

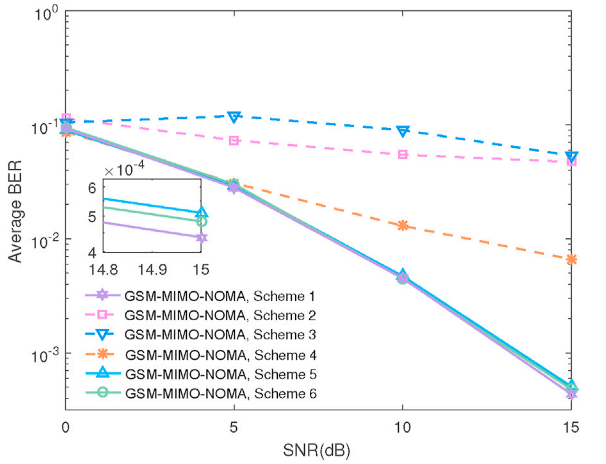

Fig. 4. Average BER performance comparison of two-user 4×4 GSMN systems under different schemes and with $K = 2$, $T = 6$, $P = 2$, $\alpha = 3$, and $R = 4$ bits/symbol.

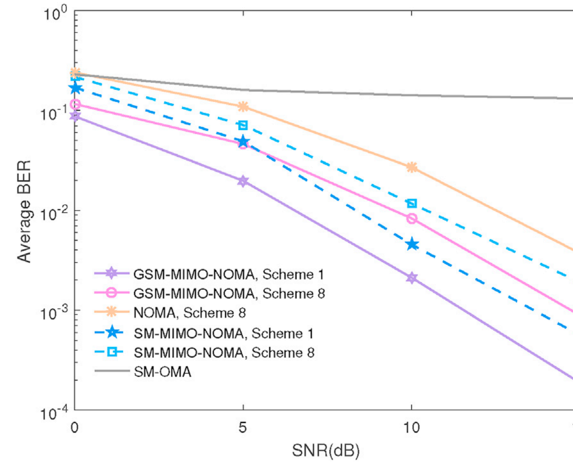

Fig. 6. Average BER performance comparison of different three-user systems with $K = 34$, $T = 4$, $P = 1$, $\alpha = 3$, and $R = 4$ bits/symbol.

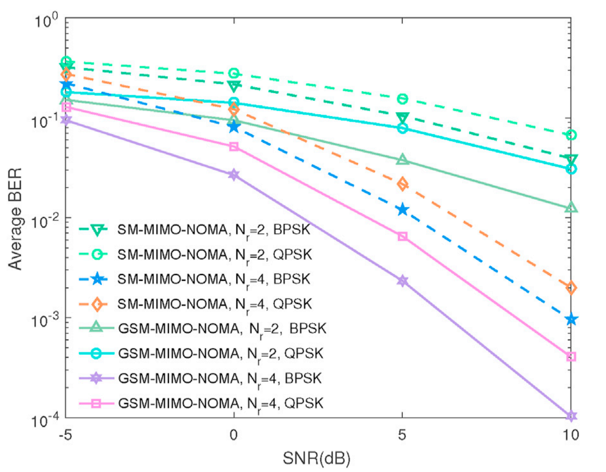

Fig. 5. Average BER performance comparison of two-user SMN/GSMN systems under different antennas and modulation orders with $K = 2$ and $T = 6$, $N_t = 4$, $P = 2$, $\alpha = 3$ and scheme 1.

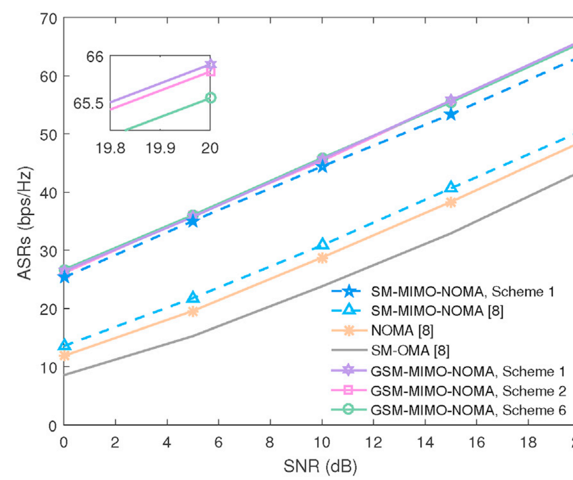

Fig. 7. ASR performance of different two-user 4×4 systems with $K = 2$, $T = 64$, $P = 5$, $\alpha = 0$, and BPSK modulation.

data is then sent sequentially through the power distribution, the transmit antenna, and the SIC modulation before reaching the receiver. The channel obeys Rayleigh distribution, and all simulation results are averaged over 10,000 random realizations.

The eight schemes investigated and compared are shown in Table 3. The BNBF grouping means that the best users will be chosen according their channel conditions as in Ref. [34]. Joint grouping was considered for the ASR maximization as in Ref. [37]. The QoS-based strategy used power allocation based on various QoS requirements, as in Refs. [35,36], and the SIC-based strategy employed power allocation to remove intra-group interference, as in Ref. [9]. Moreover, the fixed two-user strategy denoted a power ratio of $\beta_1^l : \beta_2^l = 1 : 4$, as in Ref. [32], and the fixed three-user strategy possessed a power ratio of $\beta_1^l : \beta_2^l : \beta_3^l = 2 : 3 : 45$.

Fig. 3 illustrates the average BER performance of different two-user 4×4 systems, with $P = 1$W and $\alpha = 3$. We assumed the coordinates of the BSs, u_1^t, and u_2^t were (0, 0), $(0.5\cos[(l-1)\frac{\pi}{3}], 0.5\sin[(l-1)\frac{\pi}{3}])$, and $(1.1\cos[(l-1)\frac{\pi}{3}], 1.1\sin[(l-1)\frac{\pi}{3}])$, respectively. For a fair comparison, all systems have the same data rate and the same modulation technology, as in Ref. [9].Thus, all systems utilize Quadrature Phase Shift Keying (QPSK) modulation except for SM-MIMO-NOMA systems with BPSK modulation and SM-OMA systems with 64 PSK modulation, which means the data rate of all systems is $R = 4$ bits/symbol and the modulation technology of all systems is PSK modulation. The SM-MIMO-NOMA system with Scheme 1 was superior to others, decreasing sharply from 10^{-1} to about 10^{-4}. This indicates that GSM-MIMO-NOMA systems have optimal BER performance due to TAC selection capacity. Additionally, SM-MIMO-NOMA systems utilizing Scheme 1 outperformed SM-MIMO-NOMA systems based on [9], illustrating that Scheme 1 is also effective for SM-MIMO-NOMA systems. Fig. 4 gives the average BER performance of GSM-MIMO-NOMA systems using schemes that differ from that of Fig. 3, showing that Scheme 1 was superior to other schemes. By extension, that min-cut grouping is more effective than the user grouping schemes proposed in Refs. [34, 37]. It also follows that the MaxASR strategy improves upon power allocation schemes proposed in Refs. [9,32,36], as the latter leads to a error floor presented at high SNR.

Fig. 5 illustrates the average BER performance of different two-user SM-MIMO-NOMA/GSM-MIMO-NOMA systems utilizing Scheme 1, with $N_t = 4$, $P = 2$W, and $\alpha = 3$. We assumed that the BS coordinates, u_1^t, and u_2^t were (0, 0), $(0.2\cos[(l-1)\frac{\pi}{3}], 0.2\sin[(l-1)\frac{\pi}{3}])$, and $(1\cos[(l-1)\frac{\pi}{3}], 1\sin[(l-1)\frac{\pi}{3}])$, respectively. The average BER performance increased with the number of reception antennas, and the two-user GSM-MIMO-NOMA system with BPSK modulation is superior to others.

Fig. 6 gives the average BER performance of different three-user systems with $P = 1$ W and $\alpha = 3$. We assumed the BS coordinates u_1^t, u_2^t, and

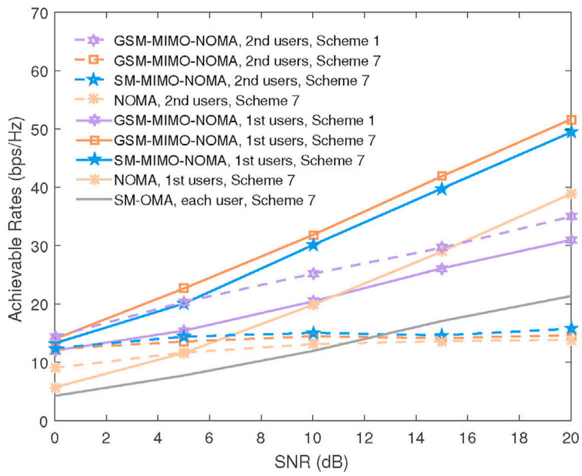

Fig. 8. Achievable rates comparison of first users and second users in different two-user 4 × 1 systems with $K = 2$, $T = 6$, $P = 5$, $\alpha = 0$, and $R = 4$ bits/symbol.

u_3^t were (0, 0), $(0.2\cos[(l-1)\frac{\pi}{2}], 0.2\sin[(l-1)\frac{\pi}{2}])$, $(0.5\cos[(l-1)\frac{\pi}{2}], 0.5\sin[(l-1)\frac{\pi}{2}])$, and $(0.8\cos[(l-1)\frac{\pi}{2}], 0.8\sin[(l-1)\frac{\pi}{2}])$, respectively. All systems had the same data rate (i.e., $R = 4$ bits/symbol) and the same modulation technology (i.e., PSK modulation) as in Ref. [9]. The 4 × 4 GSM-MIMO-NOMA systems using Scheme 1 were obviously superior to other systems, including 4 × 4 NOMA systems and 16 × 16 SM-OMA systems using Scheme. Our proposed scheme (Scheme 1) was more effective than Scheme 8 because it effectively removed intragroup interference.

Fig. 7 illustrates the ASR performance of different two-user 4 × 1 systems with $P = 5$W, $\alpha = 0$, and BPSK modulation, as in Ref. [8]. The GSM-MIMO-NOMA system was superior to the others due to the ASR increasing with the number of chosen transmit antennas. Additionally, the proposed scheme was effective for ASR maximization compared with the schemes of [35,37]. The SM-MIMO-NOMA system with Scheme 1 also had better performance than the SMN system of [8], demonstrating that the ASR performance of SMN systems also benefits from the proposed Scheme 1.

Fig. 8 gives achievable rates performance for different users in different two-user 4 × 1 systems, indicating that the acheivable rates of first users were superior to those of second users. By extension, first users with lower power allocation coefficients eliminated intragroup interference by way of the SIC procedure. GSM-MIMO-NOMA systems using Scheme 7 outperformed others in terms of achievable first-user rates. Additionally, GSM-MIMO-NOMA systems with scheme 1 have the best performance in terms of achievable second-user rates, indicating that GSM-MIMO-NOMA systems are more effective than other systems and ASR benefits from users with higher effective channel gains.

The simulation and results showed that employing GSM in a NOMA system demonstrates good performance in terms of average BER, ASR, and achievable rates. Considering the complexity and cost, a joint grouping strategy with high complexity cannot be adopted during the application of B5G mobile networks. Therefore, a low-complexity sub-optimal grouping scheme is often preferred [8]. By using the proposed graph-based user grouping strategy combined with power allocation optimization, performance is proven to be ensured or improved. We have also shown that graph theory is a useful tool for analyzing the min-cut user grouping problem; we expect this theory to attract more attention.

Table 4
Complexity of different user grouping strategies in GSM-MIMO-NOMA systems with $N = KT = 12$ users.

K	T	Joint grouping	Min-cut grouping
2	6	7484 400	40
3	4	591 360	27
4	3	7484 400	20

5.2. *Complexity discussion*

Conventional joint grouping involves $\prod_{i=1}^{T}\left[{}_{(N\ (i\ 1)K)}C_K-(i-1)K)\right] = \frac{(KT)!}{K^T}$ possibilities [37], but min-cut grouping is reduced to $K\sum_{i=1}^{T-1}[T-(i-1)C_1]$ possibilities by computing all the K-dimensional mutual gains simultaneously. Before grouping, there are $\dot{T}$ initial sets and each initial set has $\dot{K}$ users. After grouping, there are $\dot{T}$ groups with $\dot{K}$ users each. The complexity of different user grouping strategies are shown in Table 4, where the proposed min-cut grouping is compared with conventional joint grouping. Compared to a joint grouping strategy with high complexity, our proposed suboptimal user grouping algorithm has lower complexity while being effective for the proposed GSM-MIMO-NOMA systems and allowing good performance to be obtained. Thus, a tradeoff between complexity and optimal solution is achieved.

6. Conclusions

In this paper, we have proposed a GSM-MIMO-NOMA system to further improve the performance of SM-MIMO-NOMA systems, where a TAC is selected rather than only one transmit antenna. To show the superiority of the coding method, we compared BER performance under different modulation methods. Through simulation, we compared the BERs of SM-MIMO-NOMA and GSM-MIMO-NOMA systems, verifying the effectiveness of our proposed GSM method. The effectiveness of our proposed algorithm was verified by simulating the sum rate of users. In addition, analyzed the impact of dynamic resource allocation strategies on the performance of downlink SM-MIMO-NOMA/GSM-MIMO-NOMA systems with two or more users in one group. For a fair comparison, we considered two-user and three-user SM-MIMO-NOMA/GSM-MIMO-NOMA schemes during our simulations, showing that significant performance enhancement can be achieved by using the proposed schemes. We found that GSM-MIMO-NOMA systems with min-cut grouping and a MaxASR strategy had better performance than other schemes. Therefore, our proposed GSM-MIMO-NOMA schemes achieved an attractive complexity-optimality tradeoff. In the future, we will consider the impact of the inter-group interference and design a heuristic algorithm-based power allocation strategy for GSMN systems.

Declaration of competing interest

We declare that we do not have any commercial or associative interest that represents a conflict of interest in connection with the work submitted.

Acknowledgements

This work was supported by the National Key Research and Development Program of China (Grant No. 2019YFC1511300), the National Natural Science Foundation of China (Grant No. U21A20447 and 61971079), the Basic Research and Frontier Exploration Project of Chongqing (Grant No. cstc2019jcyj-msxmX0666), the Innovative Group Project of the National Natural Science Foundation of Chongqing (Grant No. cstc2020jcyj-cxttX0002)and the Regional Creative Cooperation Program of Sichuan (2020YFQ0025).

References

[1] Y. Zhou, L. Tian, L. Liu, Y. Qi, Fog computing enabled future mobile communication networks: a convergence of communication and computing, IEEE Commun. Mag. 57 (5) (2019) 20–27.
[2] Y. Zhou, L.W. Ling Liu, J.W. Ning Hui, Xinyu Cui, Service-aware 6g: an intelligent and open network based on the convergence of communication, computing and caching, Digit. Commun. Networks 6 (3) (2020) 253–260.

[3] L. Dai, B. Wang, Y. Yuan, S. Han, I. Chih-Lin, Z. Wang, Non-orthogonal multiple access for 5G: solutions, challenges, opportunities, and future research trends, IEEE Commun. Mag. 53 (9) (2015) 74–81, https://doi.org/10.1109/MCOM.2015.7263349.

[4] A. Morgado, K.M.S. Huq, S. Mumtaz, J. Rodriguez, A survey of 5G technologies: regulatory, standardization and industrial perspectives, Digit. Commun. Netw. 4 (2) (2018) 87–97, https://doi.org/10.1016/J.DCAN.2017.09.010.

[5] X. Liu, H. Ding, S. Hu, Uplink resource allocation for noma-based hybrid spectrum access in 6g-enabled cognitive internet of things, IEEE Internet Things J. (2020), https://doi.org/10.1109/JIOT.2020.3007017, 1–1.

[6] P. Yang, J. Zhu, Y. Xiao, Z. Chen, Antenna selection for MIMO system based on pattern recognition, Digit. Commun. Netw. 5 (1) (2019) 34–39, https://doi.org/10.1016/J.DCAN.2018.10.001.

[7] M.D. Renzo, H. Haas, P.M. Grant, Spatial modulation for multiple-antenna wireless systems: a survey, IEEE Commun. Mag. 49 (12) (2011) 182–191, https://doi.org/10.1109/MCOM.2011.6094024.

[8] X. Wang, J. Wang, L. He, Z. Tang, J. Song, On the achievable spectral efficiency of spatial modulation aided downlink non-orthogonal multiple access, IEEE Commun. Lett. 21 (9) (2017) 1937–1940, https://doi.org/10.1109/LCOMM.2017.2707068.

[9] X. Zhu, Z. Wang, J. Cao, NOMA-based spatial modulation, IEEE Access 5 (99) (2017) 3790–3800, https://doi.org/10.1109/ACCESS.2017.2688019.

[10] X. Wang, J. Wang, L. He, J. Song, Spectral efficiency analysis for downlink NOMA aided spatial modulation with finite alphabet inputs, IEEE Trans. Veh. Technol. 66 (11) (2017) 10562–10566, https://doi.org/10.1109/TVT.2017.2737327.

[11] J. Wang, S. Jia, J. Song, Generalised spatial modulation system with multiple active transmit antennas and low complexity detection scheme, IEEE Trans. Wireless Commun. 11 (4) (2012) 1605–1615, https://doi.org/10.1109/TWC.2012.030512.111635.

[12] Y. Xiao, Z. Yang, L. Dan, P. Yang, L. Yin, W. Xiang, Low-complexity signal detection for generalized spatial modulation, IEEE Commun. Lett. 18 (3) (2014) 403–406, https://doi.org/10.1109/LCOMM.2013.123113.132586.

[13] A. Younis, N. Serafimovski, R. Mesleh, H. Haas, Generalised spatial modulation, in: Proc. 2010 Conf. Rec. 44th Asilomar Conf. Signals, Syst. Computers, Pacific Grove, CA, USA, 2010, pp. 1–5, https://doi.org/10.1109/ACSSC.2010.5757786.

[14] P. Ju, M. Zhang, X. Cheng, C. Wang, L. Yang, Generalized spatial modulation with transmit antenna grouping for correlated channels, in: Proc. 2016 IEEE Int. Conf. Commun., Kuala Lumpur, Malaysia, 2016, pp. 1–6, https://doi.org/10.1109/ICC.2016.7511626.

[15] Z. Hong, G. Li, Y. Xu, X. Zhou, User grouping and power allocation for downlink NOMA-based quadrature spatial modulation, IEEE Access 8 (1) (2020) 38136–38145, https://doi.org/10.1109/ACCESS.2020.2974663.

[16] Z. Ding, F. Adachi, H.V. Poor, The application of MIMO to non-orthogonal multiple access, IEEE Trans. Wireless Commun. 15 (1) (2016) 537–552, https://doi.org/10.1109/TWC.2015.2475746.

[17] Y.-R. Tsai, H.-A. Wei, Quality-balanced user clustering schemes for non-orthogonal multiple access systems, IEEE Commun. Lett. 22 (1) (2018) 113–116, https://doi.org/10.1109/LCOMM.2017.2766618.

[18] H. Li, F. Fang, Z. Ding, Joint resource allocation for hybrid NOMA-assisted MEC in 6G networks, *Digit. Commun. Netw.* to be published. doi: 10.1016/J.DCAN.2020.05.005.

[19] Y. Liu, M. Derakhshani, S. Lambotharan, Outage analysis and power allocation in uplink non-orthogonal multiple access systems, IEEE Commun. Lett. 22 (2) (2018) 336–339, https://doi.org/10.1109/LCOMM.2017.2769088.

[20] F. Fang, H. Zhang, J. Cheng, V.C.M. Leung, Energy-efficient resource allocation for downlink non-orthogonal multiple access network, IEEE Trans. Commun. 64 (9) (2016) 3722–3732, https://doi.org/10.1109/TCOMM.2016.2594759.

[21] Z. Yang, Z. Ding, P. Fan, N. Al-Dhahir, A general power allocation scheme to guarantee quality of service in downlink and uplink NOMA systems, IEEE Trans. Wireless Commun. 15 (11) (2016) 7244–7257, https://doi.org/10.1109/TWC.2016.2599521.

[22] S. Timotheou, I. Krikidis, Fairness for non-orthogonal multiple access in 5G systems, IEEE Signal Process. Lett. 22 (10) (2015) 1647–1651, https://doi.org/10.1109/LSP.2015.2417119.

[23] L. Zhu, J. Zhang, Z. Xiao, X. Cao, D.O. Wu, X.G. Xia, Joint Tx-Rx beamforming and power allocation for 5G millimeter-wave non-orthogonal multiple access networks, IEEE Trans. Commun. 67 (7) (2019) 5114–5125, https://doi.org/10.1109/TCOMM.2019.2906589.

[24] X. Sun, N. Yang, S. Yan, Z. Ding, D.W.K. Ng, C. Shen, Z. Zhong, Joint beamforming and power allocation in downlink NOMA multiuser MIMO networks, IEEE Trans. Wireless Commun. 17 (8) (2018) 5367–5381, https://doi.org/10.1109/TWC.2018.2842725.

[25] Y. Xu, G. Li, Optimal and robust interference efficiency maximization for multicell heterogeneous networks, IEEE Access 7 (99) (2019) 102406–102416, https://doi.org/10.1109/ACCESS.2019.2931863.

[26] Y. Xu, G. Li, Y. Yang, M. Liu, G. Gui, Robust resource allocation and power splitting in SWIPT enabled heterogeneous networks: a robust minimax approach, IEEE Internet Things J. 6 (6) (2019) 10799–10811, https://doi.org/10.1109/JIOT.2019.2941897.

[27] S. Liu, C. Zhang, G. Lyu, User selection and power schedule for downlink non-orthogonal multiple access (NOMA) system, in: Proc. 2015 IEEE Int. Conf. Commun. Workshop, 2015, pp. 2561–2565, https://doi.org/10.1109/ICCW.2015.7247563. London, UK.

[28] M.S. Ali, H. Tabassum, E. Hossain, Dynamic user clustering and power allocation for uplink and downlink non-orthogonal multiple access (NOMA) systems, IEEE Access 4 (99) (2016) 6325–6343, https://doi.org/10.1109/ACCESS.2016.2604821.

[29] M.S. Ali, E. Hossain, D.I. Kim, Non-orthogonal multiple access (NOMA) for downlink multiuser MIMO systems: user clustering, beamforming, and power allocation, IEEE Access 5 (99) (2016) 565–577, https://doi.org/10.1109/ACCESS.2016.2646183.

[30] W.A. Al-Hussaibi, F.H. Ali, Efficient user clustering, receive antenna selection, and power allocation algorithms for massive MIMO-NOMA systems, IEEE Access 7 (99) (2019) 31865–31882, https://doi.org/10.1109/ACCESS.2019.2902331.

[31] Z. Hong, G. Li, J. Lin, Y. Xu, X. Zhou, Power allocation for downlink multiuser NOMA-based generalized spatial modulation, in: Proc. 2019 11th Int. Conf. Wireless Commun. Signal Process., 2019, pp. 1–6, https://doi.org/10.1109/WCSP.2019.8927967. Xi'an, China.

[32] F. Kara, H. Kaya, Spatial multiple access (SMA): enhancing performances of MIMO-NOMA systems, in: Proc. 2019 42nd Int. Conf. Telecommun. Signal. Process., 2019, pp. 1–6, https://doi.org/10.1109/TSP.2019.8768828. Budapest, Hungary.

[33] J.W. Kim, S.Y. Shin, V.C.M. Leung, Performance enhancement of downlink NOMA by combination with GSSK, IEEE Wireless Commun. Lett. 7 (5) (2018) 860–863, https://doi.org/10.1109/LWC.2018.2833469.

[34] T.N. Do, D.B.D. Costa, T.Q. Duong, B. An, A BNBF user selection scheme for NOMA-based cooperative relaying systems with SWIPT, IEEE Commun. Lett. 21 (3) (2017) 664–667, https://doi.org/10.1109/LCOMM.2016.2631606.

[35] Z. Yang, Z. Ding, P. Fan, N. Al-Dhahir, The impact of power allocation on cooperative non-orthogonal multiple access networks with SWIPT, IEEE Trans. Wireless Commun. 16 (7) (2017) 4332–4343, https://doi.org/10.1109/TWC.2017.2697380.

[36] T.N. Do, D.B.D. Costa, T.Q. Duong, B. An, Improving the performance of cell-edge users in MISO-NOMA systems using TAS and SWIPT-based cooperative transmissions, IEEE Trans. Green Commun., Netw. 2 (1) (2018) 49–62, https://doi.org/10.1109/TGCN.2017.2777510.

[37] J.-M. Kang, I.M. Kim, Optimal user grouping for downlink NOMA, IEEE Wireless Commun. Lett. 7 (5) (2018) 724–727, https://doi.org/10.1109/LWC.2018.2815683.

[38] L. Liang, S. Xie, G.Y. Li, Z. Ding, X. Yu, Graph-based resource sharing in vehicular communication, IEEE Trans. Wireless Commun. 17 (7) (2018) 4579–4592, https://doi.org/10.1109/TWC.2018.2827958.

[39] E. Björnson, J. Hoydis, L. Sanguinetti, Massive MIMO networks: spectral, energy, and hardware efficiency, Digit. Commun. Networks 11 (3) (2018) 154–655, https://doi.org/10.1561/2000000093.

[40] G. Michael, B. Stephen, CVX: MATLAB software for disciplined convex programming, version 2.1 [Online]. Available: http://cvxr.com/cvx/, Mar. 2014.